Proceedings of the 1998 Conference on Information Sciences and Systems

---

Volume II

Department of Electrical Engineering
Princeton University
Princeton, New Jersey 08544-5263

A System Approach to the Design of Gain-Clamped Doped-Fiber Amplifiers

Alberto Bononi and Lorenzo Barbieri
Università di Parma – Dipartimento di Ingegneria dell'Informazione – Viale delle Scienze, I-43100 Parma, Italy
phone: +39-521-905-760 fax: +39-521-905-758 – email: bononi@tlc.unipr.it, barbieri@tlc.unipr.it

Abstract— This paper provides a detailed analysis of the design of gain-clamped doped fiber amplifiers for best dynamic performance in a WDM networking environment. A simple dynamic model of the doped fiber amplifier allows us to derive explicit expressions for the small-signal transients, which help identify and optimize the most critical parameters for best dynamic performance. The most important parameter is the pump power: the larger, the better the transient response. The pump power should be chosen a few dBs above its required open-loop value, with all channels present, for the planned inversion level. In an all-optical networking scenario with input power per channel as high as -3 dBm the required pump power may well exceed 20 dBm. Thus optimization of other parameters such as laser wavelength and loop loss are important. For best dynamic performance either the loop loss should be extremely small, implying a large laser flux, or the laser gain variation in response to a perturbation should be large. Accordingly, the laser wavelength, for the data in our case study, should be placed either around 1511 nm or around 1535 nm.

I. Introduction

Doped-fiber amplifiers (DFAs) for wavelength division multiplexed (WDM) systems have a non-flat gain-versus-wavelength profile, which greatly varies because of saturation when the input power levels are large. In the design of optically amplified links for WDM applications, in which the number and the power level of the input channels may vary randomly in time as in a networking scenario, it is thus essential to stabilize the amplifier gain profile.

Several feedback control techniques have been proposed in the literature, all more or less explicitly aiming at stabilizing the average inversion of the doped-fiber amplifier. A first class uses some optical measure of inversion at the output of the amplifier to produce an error signal which electrically controls the power of either the pump or of an extra control input laser source [1]–[4]. The second class uses an all-optical feedback lasing signal sustained by the amplifier itself, which clamps the average inversion and thus the gain to the desired level [5]–[8]. The feedback is either obtained by forming a feedback fiber loop (effectively implementing a fiber ring laser), or by placing fiber gratings, acting as mirrors only at the laser wavelength, at the active fiber ends. The laser plays here the role of the extra control input laser source of the previous class. Gain clamping has also been successfully applied to semiconductor optical amplifiers [8],[9] which notoriously suffer much more than doped-fiber amplifiers from saturation-induced gain crosstalk in WDM systems.

While most of the above references deal with the steady-state analysis of gain-clamped amplifiers, a great deal of studies on their transient gain dynamics has recently appeared in the context of all-optical networks [10]–[13].

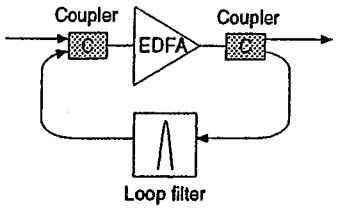

Fig. 1. Gain-clamped amplifier scheme.

This paper addresses the design of gain-clamped doped-fiber amplifiers, utilizing the simplified dynamic model of the open-loop amplifier introduced in [14],[15]. The model essentially coincides with the one in [10], where a single section is used for the doped fiber. Such a simple model allows an easy interpretation of gain clamping, and a simple study of its dynamics. Control theory techniques are used to find the values of pump power, laser power and wavelength and loop loss for optimal dynamic response.

II. Model

The gain-clamped amplifier under study is shown in Fig. 1. It is composed of a single-section DFA, with a piece of standard fiber feeding part of the output to the DFA input. Such positive feedback causes instability, and if the DFA gain is larger than the loop losses the system starts oscillating at the wavelength selected by the narrowband loop filter centered at $\lambda_l = c/\nu_l$, where c is the speed of light.

In the assumption of a two-level system for the dopant ions and an homogeneously broadened gain spectrum, the DFA can be modeled as a nonlinear dynamic system with a single state variable, namely its total number of excited ions r, called the *reservoir* [14]. If r_{max} is the total number of ions in the DFA, the normalized reservoir $x \triangleq r/r_{max}$ represents the average fraction of excited ions in the DFA, known as *average inversion*. The update equation for the reservoir, including self-saturation induced by the amplified spontaneous emission (ASE) noise is [15], [10]:

$$\dot{r}(t) = \sum_{j \in \{\mathcal{S},p,l\}} Q_j(t) \left\{1 - e^{G[r(t),\nu_j]}\right\} - \frac{r(t)}{\tau} - Q_{ASE}(r(t)) \tag{1}$$

where Q_j, $j \in \mathcal{S} \triangleq \{1,\ldots,N\}$ are the input WDM channel fluxes [photons/sec] at frequencies ν_j, Q_p the pump flux, Q_l the input laser flux, $Q_{ASE}(r)$ the output ASE flux and τ the fluorescence lifetime. $G[r,\nu_j] = B_j r - A_j$ is the logarithmic gain at frequency ν_j [14]; B_j and A_j are non-dimensional coefficients, dependent on frequency ν_j through the ions absorption and emission cross-sections [14]. We physically

interpret equation (1) as the balance between the amplifier's input and output fluxes, being the net contribution of that balance the reservoir's variation per unit time. The output flux at each frequency ν_j is obtained as $Q_j(t)e^{G[r(t),\nu_j]}$.

We then account for the optical feedback by writing the laser input flux as a delayed and attenuated version of the output flux, to which we add the ASE term over the feedback filter bandwidth $Q_{l,ASE}$:

$$Q_l(t) = \alpha\left\{Q_l(t-\tau_l)\,e^{G[r(t-\tau_l),\nu_l]} + Q_{l,ASE}[r(t-\tau_l)]\right\} \tag{2}$$

being τ_l the loop propagation delay and $0 \le \alpha \le 1$ the loop attenuation, both at laser frequency ν_l.

Equations (1)–(2) form the dynamic model of the gain-clamped amplifier. The number of state variables is now two, the second being the laser flux.

III. Steady-State Analysis

The system steady-state is obtained by letting $\dot{r}(t) = 0$ in (1) and $Q_l(t) = Q_l(t-\tau_l)$ in (2). As a result we get:

$$r_{ss} = \tau\left\{\textstyle\sum_{j\in\{\mathcal{S},p,l\}} Q_j\left[1 - e^{G(r_{ss},\nu_j)}\right] - Q_{ASE}(r_{ss})\right\} \tag{3a}$$

$$Q_l^{ss}\left[1 - \alpha\cdot e^{G(r_{ss},\nu_l)}\right] = \alpha\cdot Q_{l,ASE}(r_{ss}). \tag{3b}$$

As noted from (3b), if the ASE term in the feedback filter bandwidth is much smaller than the steady state laser flux, equation (3b) can be approximated as

$$1 - \alpha\cdot e^{G(r_{ss},\nu_l)} = 0 \tag{4}$$

which gives an explicit expression for the steady state reservoir

$$r_{ss} = \frac{\ln 1/\alpha + A_l}{B_l}. \tag{5}$$

Eq. (4) is the well-known Barkhausen criterion for steady state oscillation in a feedback noiseless system [16][1]. Since the ASE power in the feedback filter bandwidth can be made small enough by appropriately choosing the filter bandwidth, in the following we will use (5) to get the steady-state reservoir solution.

In order to get physically acceptable solutions, the laser photon flux must be non-negative. From (3a) and (4) we get:

$$Q_l^{ss} = \frac{\sum_{j\in\{\mathcal{S},p\}} Q_j\left[1 - e^{G(r_{ss},\nu_j)}\right] - \frac{r_{ss}}{\tau} - Q_{ASE}(r_{ss})}{1/\alpha - 1}. \tag{6}$$

so that the condition $Q_l^{ss} \ge 0$ gives:

$$Q_p\left[1 - e^{G(r_{ss},\nu_p)}\right] \ge \sum_{j\in\mathcal{S}} Q_j\left[e^{G(r_{ss},\nu_j)} - 1\right] + \frac{r_{ss}}{\tau} + Q_{ASE}(r_{ss}), \tag{7}$$

which we interpret either as a lower bound on pump flux or as an upper bound on input fluxes. With the sign of equality, (7) represents a hyperplane bounding the limit values of the variables Q_p and $\{Q_j\}$, $j \in \mathcal{S}$.

[1] The oscillation condition on the signal phase is neglected here since the lasing modes form a continuum, because the loop delay τ is usually more than 6 orders of magnitude larger than the mode wavelength.

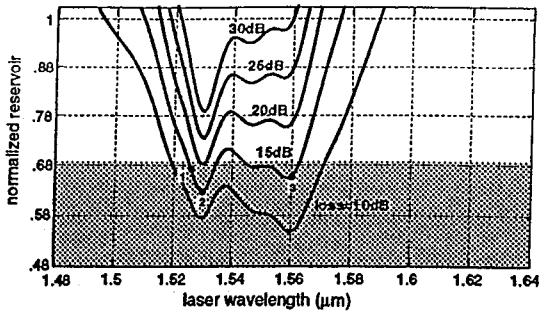

Fig. 2. Steady-state average inversion $x \triangleq r_{ss}/r_{max}$ vs laser wavelength, with loop loss as a parameter.

Let's now consider a numerical example. The erbium DFA (EDFA) parameters used are: pump wavelength $\lambda_p = 1480$ nm; fluorescence time $\tau = 10.5$ ms; erbium concentration $\rho = 1.14 \times 10^{24}$ ions/m^3; overlap factor $\Gamma = 0.5$; effective core area $A_{eff} = 5.12 \times 10^{-12}$ m^2; EDFA length $L = 35$ m; cross-section values taken from fitted lorentzian curves in [[17], table 4.2, p. 299] with $\sigma^e_{max} = 5.8 \times 10^{-25}$ m^2 and $\sigma^a_{max} = 5.3 \times 10^{-25}$ m^2. The above parameters are related to the A_j and B_j factors as: $A_j = \rho\Gamma\sigma^a_j L$ $B_j = \Gamma(\sigma^e_j + \sigma^a_j)/A_{eff}$. The WDM system is composed of 8 channels with equal input power per channel $P_{in/ch}$ at frequencies chosen according to the ITU-T standard between 192.8 THz (1554.9 nm) and 193.5 THz (1549.3 nm), with 100 GHz (0.8 nm) spacing.

Fig. 2 shows the normalized reservoir x vs laser wavelength as obtained from (5), with loop loss $1/\alpha$ as a parameter. Choosing $P_p = 18$ dBm and $P_{in/ch} = -10$ dBm in (7) gives an upper bound on r_{ss}, shown by the shaded area in the figure: to satisfy both (5) and (7) the loop loss cannot exceed 20 dB in the example.

Select for example a loop loss of 15 dB. To check the effect of varying the laser wavelength, we choose wavelengths $\lambda_{l1} = 1526$ nm, $\lambda_{l2} = 1530$ nm, and $\lambda_{l3} = 1560$ nm, obtaining the three distinct values of the average inversion, and hence of the gain profile, marked in Fig. 2. With the above values of the reservoir, we show in Fig. 3a the effect of varying the signal input power $P_{in/ch}$ for a fixed pump power $P_p = 18$ dBm: with decreasing channel fluxes, the laser flux grows to consume the excess reservoir excited ions that would otherwise result. We see that input powers below -22 dBm/ch do not influence the laser power, which in this case has about 16 dBm power and is the only cause of EDFA saturation. Fig. 3b shows the maximum output laser flux, obtained in the absence of channel fluxes ($P_{in/ch} = 0$), for varying pump power: being the gain (i.e., the average inversion) clamped, the laser power increases with pump power to consume the excess reservoir excited ions provided by a more powerful pump. Note from both figures that the laser power is minimized by choosing λ_l, in the allowed lasing range, so that the value of the stabilized reservoir is maximum, corresponding to maximum gain at the laser wavelength.

Finally, a lower bound on the pump power to ensure the existence of the laser oscillation in all possible static configurations of the WDM system is obtained from (7) by

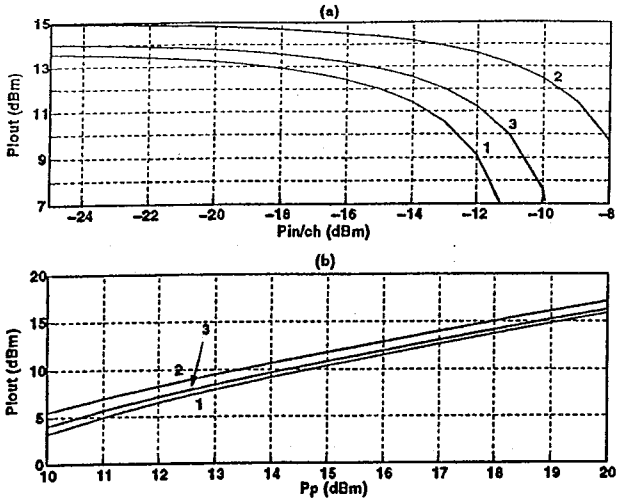

Fig. 3. Laser output power versus (a) input channel power, for fixed $P_p = 18$ dBm; (b) pump power, without input WDM channels.

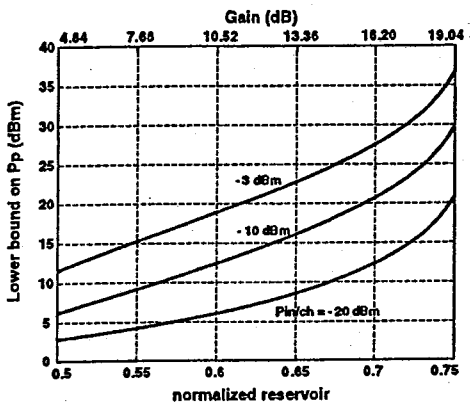

Fig. 4. Lower bound on pump power versus average inversion, with input power per channel as a parameter.

imposing the equality sign when all the WDM channels are present. Such a minimum pump level is the one needed by an open-loop amplifier to guarantee the required gain level and profile with all channels present. Fig. 4 shows such bound versus normalized steady-state reservoir, with input power per channel $P_{in/ch}$ (for our 8 channel WDM system) as a parameter. The reservoir fixes the gain profile and level, which in the middle of the comb has the dB values indicated in the upper "Gain" axis. Such curves do not depend on laser parameters, since they are obtained as limiting cases at which $Q_l = 0$. We observe that for a typical interamplifier loss of 10–15 dB the average inversion is around 0.63. The pump lower bound is below 10 dB for signal levels of -20 dBm/ch, below 16 dB for -10 dBm/ch, and as high as 23 dB for a typical value for all-optical networks such as -3 dBm/ch. This means that a very large pump value is already required for open-loop EDFAs to guarantee the required gain and profile. When we clamp the gain, we have to provide more pump to sustain the laser oscillation. We will show in the next section that the amount of required extra pump to achieve a satisfactory dynamic behavior is usually a few dB larger than the lower bound.

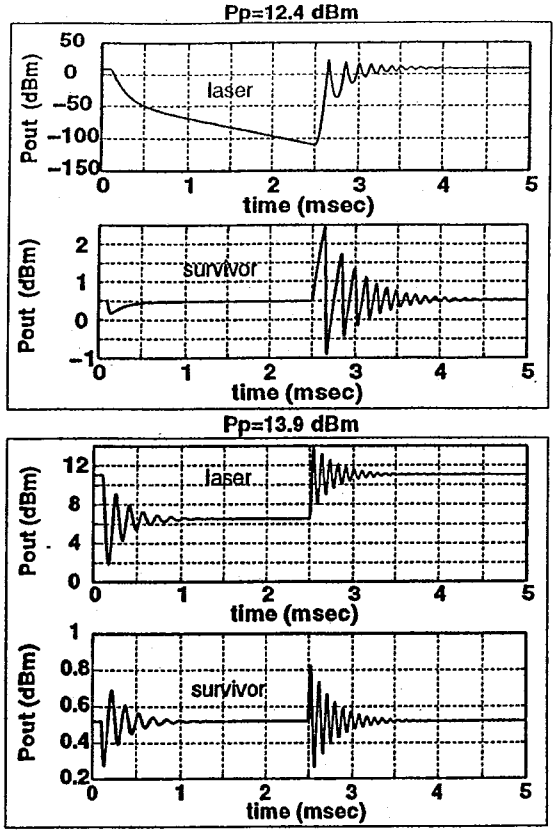

Fig. 5. Laser (top) and surviving channel (bottom) output power time response to a 7 channel add/drop sequence, with $P_{in/ch} = -10$ dBm, $\lambda_l = 1530$ nm, $\tau_l = 2\,\mu s$.

IV. Design for Optimal Dynamic Performance

In the design of the gain-clamped amplifier we have a constraint on the required gain level and gain-vs-wavelength profile for the WDM channels, of which we know the number and the input power level $P_{in/ch}$. Once the profile is stabilized by gain clamping, gain equalization can optionally be achieved by using a suitable passive optical filter [18]. Considering that the major cost is due to the large pump power in the DFA, our target is to stabilize a given gain profile, for given input channels and required gain level, by *minimizing* the required pump power.

Since a one-to-one relation exists between gain profile and reservoir value, system specifications fix the required value for r_{ss} at steady state. Given r_{ss}, laser wavelength λ_l and loop loss are related by the Barkhausen criterion (5). We have one degree of freedom in the choice between loss and λ_l.

Another degree is available with the selection of the pump power, for which a lower bound to ensure the existence of the laser oscillation was obtained in the previous section.

To understand the effect of choosing the pump level very close to its lower bound (Cfr Fig. 4) on the dynamic response of the clamped amplifier, we note that in this case the laser level is very small. When a channel drop occurs, a long "switch on" transient takes place, giving a slow response and large overshoots on the surviving channels.

Fig. 5a refers to a system with average inversion $x = 0.6$, $P_{in/ch} = -10$ dBm, $\lambda_l = 1530$ nm, and pump power

$P_p = 12.4$ dBm corresponding to its lower bound. The figure shows a double transient in our WDM system: before time 0 there is only 1 active channel, and at time 0.1 ms the remaining 7 channels are added. Being the pump power at its lower bound, when all channels are present the laser switches off. After some fraction of ms the laser power is negligible compared to the WDM channels and does not influence the dynamics of the surviving channel anymore. At time 2.5 ms the 7 channels are dropped. Clearly, since the laser is essentially off, a long (0.2 ms) switch-on transient occurs, and large (2 dB) power excursions show up on the surviving channel, with a long ringing. It takes more than 1.5 ms for the system to settle to the new steady-state. Fig. 5b shows what happens if the pump is chosen 1.5 dB above the lower bound, $P_p = 13.9$ dBm. In such case a laser oscillation (6.5 dBm) is present even after the initial 7-channel add, so that the subsequent 7-channel drop causes a transient in the system that settles after a little more than 0.5 ms, with a power excursion on the surviving channel of only 0.25 dB.

From this we learn that a little more pump power with respect to its lower bound helps improve the dynamic response.

To better quantify the dynamic behavior and thus finalize the design criteria, we now perform a small-signal analysis, leading to explicit formulae for the relaxation oscillations [19].

V. Small-Signal Analysis: Relaxation Oscillations

In this section we slightly perturb the equilibrium point and find an explicit solution of the linearized system response. Our objective is to obtain explicit expressions of the decay rate and relaxation oscillation frequency, and see how they relate to our free parameters in order to design the system for shortest transient duration. We carry on the analysis without the ASE contributions in the model equations (1) and (2).

Let the perturbed input and state values be:

$$\begin{cases} Q_j(t) \triangleq Q_j^{ss} + \Delta Q_j\, u(t), & j = 1,\dots,N \\ r(t) \triangleq r_{ss} + r_\Delta(t), & r_\Delta(t) \ll r_{ss} \\ Q_l(t) \triangleq Q_l^{ss} + Q_\Delta(t), & Q_\Delta(t) \ll Q_l^{ss} \end{cases}$$

where $u(t)$ is the step function. Using such values in (1), approximating the amplifier's exponential gain as $e^{G(r_{ss},\nu_j)}[1 + B_j r_\Delta(t)]$ we obtain for $t \geq 0$:

$$\begin{aligned} \dot r_\Delta(t) = & -\tfrac{r_\Delta(t)}{\tau} + \textstyle\sum_{j\in\{s,p\}} \Delta Q_j \left[1 - e^{G(r_{ss},\nu_j)}\right] + \\ & + Q_\Delta(t)\left[1 - e^{G(r_{ss},\nu_l)}\right] - \textstyle\sum_{j\in\{s,p,l\}} Q_j(0^+) \\ & e^{G(r_{ss},\nu_j)} B_j \cdot r_\Delta(t) - e^{G(r_{ss},\nu_l)} B_l\, Q_\Delta(t)\, r_\Delta(t) \end{aligned} \tag{8}$$

where $Q_j(0^+) = Q_j^{ss} + \Delta Q_j$ for signals, and $Q_l(0^+) = Q_l^{ss}, Q_p(0^+) = Q_p$. If we define:

$$\begin{cases} \frac{1}{\tau_c} \triangleq \frac{1}{\tau} + \sum_{j\in\{s,p,l\}} Q_j(0^+) e^{G(r_{ss},\nu_j)} B_j \\ K \triangleq \sum_{j\in\{s,p\}} \Delta Q_j \left[1 - e^{G(r_{ss},\nu_j)}\right], \end{cases} \tag{9}$$

we write equation (8) as:

$$\begin{aligned} \dot r_\Delta(t) = & -\tfrac{r_\Delta(t)}{\tau_c} + Q_\Delta(t)\left[1 - e^{G(r_{ss},\nu_l)}\right] \\ & - e^{G(r_{ss},\nu_l)} B_l\, Q_\Delta(t)\, r_\Delta(t) + K. \end{aligned} \tag{10}$$

Similarly, from equation (2) we get:

$$Q_\Delta(t) = Q_\Delta(t-\tau_l) + Q_l^{ss} B_l r_\Delta(t-\tau_l) + B_l Q_\Delta(t-\tau_l) r_\Delta(t-\tau_l). \tag{11}$$

Since we are considering small perturbations with respect to steady state solutions, we will neglect cross products between r_Δ and Q_Δ. Taking the Laplace transforms of equations (10) and (11), and using a first-order Padé rational approximation for the delay term $e^{-\tau_l s} \simeq \frac{1-\tau_l s/2}{1+\tau_l s/2}$ we get:

$$\begin{cases} (s + \frac{1}{\tau_c}) R_\Delta(s) & + & (1/\alpha - 1) Q_\Delta(s) & = & \frac{K}{s} \\ Q_l^{ss} B_l (s\,\frac{\tau_l}{2} - 1) R_\Delta(s) & + & s\,\tau_l Q_\Delta(s) & = & 0 \end{cases} \tag{12}$$

being $R_\Delta(s)$, $Q_\Delta(s)$ the Laplace transforms of $r_\Delta(t)$, $Q_\Delta(t)$ respectively. The associated characteristic equation is:

$$s^2 + \left[\frac{1}{\tau_c} - \frac{Q_l^{ss}}{2} B_l (1/\alpha - 1)\right] s + \frac{Q_l^{ss} B_l}{\tau_l} (1/\alpha - 1) = 0$$

whose roots, when the determinant is negative, are $s_{1,2} = -\gamma \pm j\omega$, where the decay rate γ and the relaxation-oscillation frequency ω are:

$$\begin{cases} \gamma = \frac{1}{2}\left[\frac{1}{\tau_c} - \frac{Q_l^{ss}}{2} B_l (1/\alpha - 1)\right] \\ \omega = \frac{1}{2}\sqrt{4\,\frac{Q_l^{ss} B_l}{\tau_l}(1/\alpha - 1) - \left[\frac{1}{\tau_c} - \frac{Q_l^{ss}}{2} B_l (1/\alpha - 1)\right]^2}. \end{cases} \tag{13}$$

The perturbed solution finally is:

$$\begin{cases} r(t) = r_{ss} + K\,\frac{e^{-\gamma t}}{\omega} \cdot \sin \omega t \\ Q_l(t) = Q_l^{ss} + \frac{K}{1/\alpha - 1}\left\{1 - \frac{e^{-\gamma t}}{\omega}\left\{[\gamma + \right.\right. \\ \qquad \left.\left. + Q_l^{ss} B_l (1/\alpha - 1)]\sin \omega t + \omega \cos \omega t\right\}\right\}. \end{cases} \tag{14}$$

In Fig. 6 the small-signal solution (14) is compared to the exact solution of (1),(2) when 7 out of 8 low-power channels are dropped. The prediction is quite good, and starts to fail only when the added/dropped power variations are significant with respect to the total steady-state input power. Fig. 7 summarizes the results in (13) by giving the root locus $s_{1,2} = -\gamma \pm j\omega$ on the complex plane, as the laser wavelength λ_l is swept across its allowed range, starting from $\lambda_l = 1511.35$ nm (points marked with a cross) up to $\lambda_l = 1640$ nm (white circles). The sweep direction is marked by arrows. Since the inversion is clamped at $x = 0.6$, at each point the loss changes according to (5) and the values are shown for the marked points. Two different loci are shown for two distinct values of the pump power. As seen, increasing the pump from 13.9 to 18 dBm gives larger values of both decay rate (faster decay) and relaxation frequency (faster oscillations), in accord with our previous observation in Fig. 5. We also note that an 18 dBm pump may give real roots, in which case the fastest settling time is obtained by choosing coincident real roots. For both pump values,

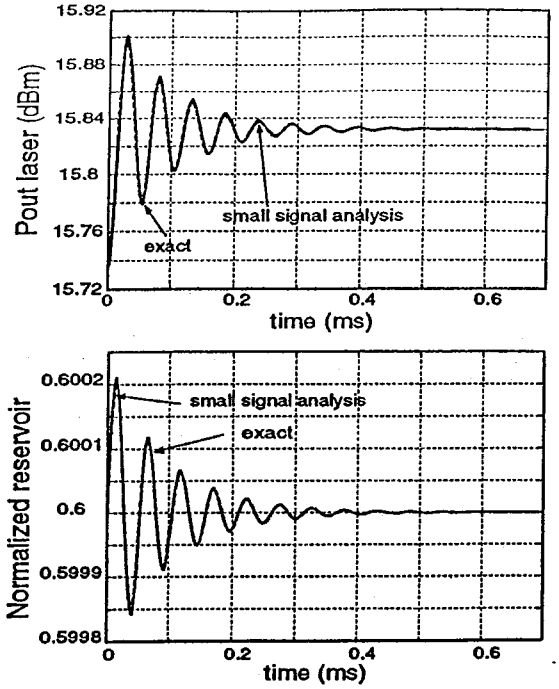

Fig. 6. Output laser power (top) and average inversion (bottom) dynamic response: small-signal solution (solid) and exact solution (dashed). Data: $P_p = 18$ dBm, $P_{in/ch} = -20$ dBm, $x = 0.6$; $\lambda_l = 1530$ nm, $\tau_l = 2$ μs).

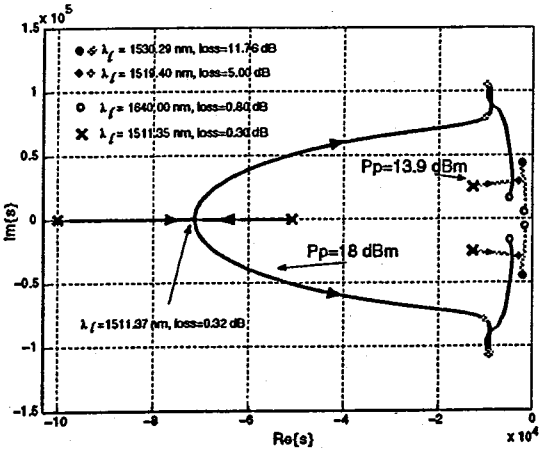

Fig. 7. Root locus $s_{1,2}$ of the small-signal characteristic equation as λ_l is swept across its allowed range, for $P_{in/ch} = -20$ dBm, $x = 0.6$ and two pump values: (black) 18 dBm; (grey) 13.9 dBm.

the transient duration is minimized by choosing λ_l around 1511 nm, where the loss is extremely low and γ is largest; this however corresponds to unrealistically small loop loss (0.3 dB). With achievable loop loss values larger than, say, 5 dB (diamond points), the roots are complex in both cases.

We write in more detail the decay rate to check its dependence on laser wavelength. From the first of (13), and the first of (9) we get:

$$\gamma = \frac{1}{2}\left[\frac{1}{\tau} + Q_p\, e^{G(r_{ss},\nu_p)} B_p + \frac{Q_l^{ss}}{2} B_l (1/\alpha + 1) + \sum_{j\in\mathcal{S}} \left(Q_j^{ss} + \Delta Q_j\right) e^{G(r_{ss},\nu_j)} B_j\right] \quad (15)$$

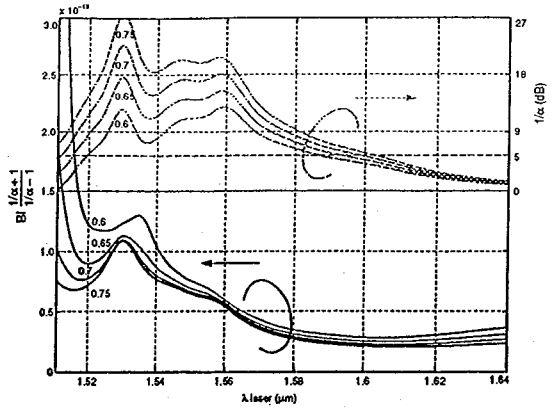

Fig. 8. Plot of term F versus laser wavelength λ_l for different required inversion levels x, with $P_{in/ch} = -20$ dBm. Top grey curves and right axis: loss vs λ_l.

As seen from (15) and (6), the only dependence of γ on λ_l comes through the term $F \triangleq B_l \frac{1/\alpha+1}{1/\alpha-1}$ for a planned value of r_{ss}. This term should be large for fast oscillation decay. Maximizing B_l maximizes the gain variation induced by a given reservoir variation [2], and minimizing the loss maximizes the input laser flux in photons/s as per (6), so that the laser reaction to the add/drop, coming from a decrease/increase of the ions consumed in the reservoir, is improved in speed.

The term F is plotted in Fig. 8 for different values of inversion x. Obviously it tends to infinity when α tends to one. Thus one should choose the loop loss as small as possible (largest laser flux) for fastest dynamic response. The loss vs λ_l curves for given inversion x (i.e., the stabilized gain profiles) are also shown in the figure. It is interesting to note that for feasible loop losses above, say, 5 dB the term F varies within a factor of 4, which may be significant since $r(t)$ varies exponentially with it. Good laser wavelength ranges for the data in our case study are around 1511 nm, where the loss tends to one, and in a small range around 1535 nm where B_l is maximum.

It has been pointed out in [20] that the best noise figure is obtained for lowest input laser flux, giving maximum inversion at the input. Lowest input laser flux corresponds to largest laser gain, and thus 1535 nm is best for both noise figure and dynamic response.

However, the principal noise figure degradation comes from the WDM signal loss at the input coupler, which should therefore be mimimum. In this respect, either we accept a large loop loss, e.g. with a standard 90/10 coupler, or we use a laser well out of band, so that a wavelength multiplexer can be used, which introduces minimum input signal loss, without too much increase in the laser loop loss.

Also note that, contrary to what stated in [20], a gain-clamped amplifier can only degrade the noise figure with respect to its open-loop counterpart, since without clamping the inversion is always larger when not all WDM channels are present (the laser consumes the extra inversion in the absence of some of the WDM channels).

The last quantity of interest in the transient analysis is

[2] Recall that each input laser photon consumes $e^{B_l r_{ss} - A_l}$ reservoir ions.

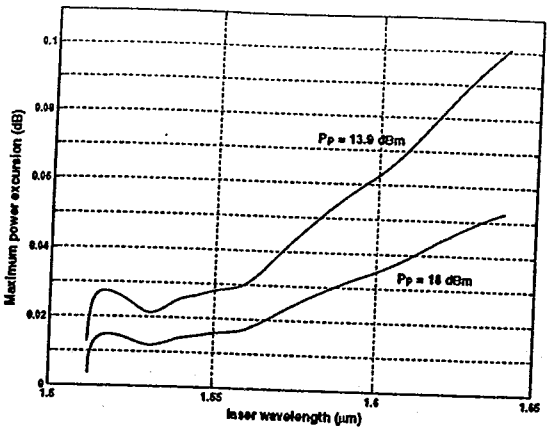

Fig. 9. Maximum power excursion on surviving channel for 7 out of 8 channel add/drop versus laser wavelength, for two pump power values. Parameters: $x = 0.6$; $P_{in/ch} = -20$ dBm.

the power excursion on surviving channels. Since the output power at channel j is $P_j^{out} = Q_j h\nu_j e^{G(r_{ss},\nu_j)}$, the dB power excursion on channel j is:

$$\Delta P_{j\,|\,dB} \triangleq 10\log_{10}\frac{P_j(r_{ss}+r_\Delta(t))}{P_j(r_{ss})} \simeq 4.34 B_j r_\Delta(t). \quad (16)$$

By setting to zero the derivative of r_Δ, the maximum reservoir excursion is obtained at $\hat{t} = \frac{atan(\omega/\gamma)}{\omega}$. Fig. 9 shows the maximum power excursion $\Delta P_{j\,|\,dB} \simeq 4.34 B_j \frac{K}{\omega} e^{-\gamma\hat{t}} \cdot \sin\omega\hat{t}$ of the single surviving channel to an add/drop of 7 channels, as a function of laser wavelength. We note that the power excursion can be reduced by increasing the pump power. In this case the band below 1520 nm is optimal. Although these results were obtained reasoning on the small-signal response, the conclusions still hold true in the large signal case.

VI. Conclusions

We have provided a detailed analysis of the design of gain-clamped DFAs in a WDM networking environment. The simplicity of the DFA model allowed us to derive explicit expressions for the small-signal transients, which helped identify and optimize the critical parameters for best dynamic performance. The most important parameter is the pump power: the larger, the better the transient response. The pump power should be chosen a few dBs above its required open-loop value, with all channels present, for the planned inversion level. In an all-optical networking scenario with input power per channel as high as -3 dBm the required pump power may well exceed 20 dBm. Thus optimization of other parameters such as laser wavelength or loop loss may be of importance to allow lower pump values. We have shown that, for any pump level, when the loop loss is very small the laser becomes extremely large, and this gives the best dynamic performance. For the data in our case study, the laser should be placed around 1511 nm. However obtaining such low loss values is hard, and for practical loss values the laser wavelength for fastest response should be placed at the peak of the clamped profile, 1535 nm in our case.

Acknowledgments

This work was supported partly by the European Community under INCO-DC project No. 950959 "DAWRON", and partly by a grant from CSELT. Prof. Aurelio Piazzi is gratefully acknowledged for suggesting the Padé approximation of the delay term. The first author wishes to thank Prof. Leslie Rusch for rekindling his interest in optical amplifiers.

References

[1] C. R. Giles, E. Desurvire, and J. R. Simpson, "Transient gain and crosstalk in erbium-doped fiber amplifier," *Opt. Lett.*, vol. 14, pp. 880–881, 1989.

[2] K. Motoshima, K. Shimizu, K. Takano, and T. Mizuochi, "EDFA with dynamic gain compensation for multiwavelength transmission systems," in *Proc. OFC '94*, San Jose, CA, pp. 191–192, Feb. 1994.

[3] F. Shehadeh, R. S. Vodhanel, C. Gibbons, and M. Ali, "Comparison of gain control techniques to stabilize EDFAs for WDM networks," in *Proc. OFC '96*, San Jose, CA, pp. 190–191, Feb. 1996.

[4] J. L. Zyskind, A. K. Srivastava, Y. Sun, J. C. Ellson, G. W. Newsome, R. W. Tkach, A. R. Chraplyvy, J. W. Sulhoff, T. A. Strasser, J. R. Pedrazzani and C. Wolf, "Fast link control protection for surviving channels in multiwavelength optical networks," in *Proc. ECOC '96*, Oslo, Norway, vol. 5, pp. 49–52, 1996.

[5] M. Zirngibl, "Gain control in erbium-doped fiber amplifiers by an all-optical feedback loop," *Electron. Lett.*, vol. 27, pp. 560–561, 1991.

[6] E. Delevaque, T. Georges, J. F. Bayon, M. Monerie, P. Niay, and P. Berage, "Gain control in erbium-doped fiber amplifiers by lasing at 1480 nm with photoinduced Bragg gratings written on the fiber ends," *Electron. Lett.*, vol. 29, pp. 1112–1114, 1993.

[7] J. F. Massicott, S. D. Wilson, R. Wyatt, J. R. Armitage, R. Kashyap and D. Williams, "1480 nm pumped erbium doped fiber amplifier with all-optical automatic gain control," *Electron. Lett.*, vol. 30, pp. 962–964, 1994.

[8] J. C. Simon, P. Doussiere, P. Lamouler, I. Valiente, F. Riou, "Travelling wave semiconductor optical amplifier with reduced nonlinear distortions," *Electron. Lett.*, pp. 49–50, Jan. 1994.

[9] G. Soulage, A. Jourdan, P. Doussiere, G. da Loura, "Clamped-gain SOA gates as multiwavelength space switches," in *Proc. OFC '95*, San Diego, CA, pp. 9–10, Feb. 1995.

[10] R. Lebref, B. Landousies, T. Georges, and E. Delevaque, "Study of power transients in EDFA with gain stabilisation by a laser effect," *Electron. Lett.*, vol. 33, pp. 191–193, Jan. 1997.

[11] D. H. Richards, M. A. Ali, and J. L. Jackel, "A theoretical investigation of dynamic automatic gain control in multi-channel EDFA cascades," in *Proc. ECOC '97*, Edinburgh, UK, pp. 47–50, Sep. 1997.

[12] J. Chung, and S. Y. Kim, "Dynamic performance of the all-optical gain-controlled EDFA cascade in multi-wavelength add/drop networks," in *Proc. ECOC '97*, Edinburgh, UK, pp. 139–142, Sep. 1997.

[13] G. Luo, J. L. Zyskind, Y. Sun, A. K. Srivastava, J. W. Sulhoff, C. Wolf, and M. A. Ali, "Performance degradation of all-optical gain-clamped EDFAs due to relaxation oscillations and spectral hole burning in amplified WDM networks," *Photon. Technol. Lett.*, vol. 9, pp. 1346–1348, Oct. 1997.

[14] A. Bononi, L. A. Rusch, and L. Tancevski, "Simple dynamic model of fibre amplifiers and equivalent electric circuit" *Electron. Lett.*, vol. 33, no. 22, pp. 1887-1888, Oct. 1997.

[15] A. Bononi, L. Barbieri, and L. A. Rusch, "Using SPICE to simulate gain dynamics in doped-fiber amplifier chains", presented at *OFC '98*, San Jose, CA, workshop 204 "Transmission modelling simulation tools", Monday February 23, 1998.

[16] J. Millman, *Microelectronics*, McGraw-Hill, 1979

[17] E. Desurvire, *Erbium-doped fiber amplifiers*. Wiley, 1994.

[18] R. Lebref, B. Landousies, T. Georges, and E. Delevaque, "Theoretical study of the gain equalization of a stabilized gain EDFA for WDM applications," *J. Lightwave Technol.*, vol. 15, pp. 766–770, May 1997.

[19] A. E. Siegman, *Lasers*, University Science Books, 1986

[20] M. Cai, X. Liu, J. Cui, P. Tang, and J. Peng, "Study on noise characteristic of gain-clamped erbium-doped fiber-ring lasing amplifier," *Photon. Technol. Lett.*, vol. 9, pp. 1093–1095, Aug. 1997.